Spontaneous spatiotemporal waves of gene expression from biological clocks in the leaf

Spontaneous spatiotemporal waves of gene expression from biological clocks in the leaf

Bénédicte Wenden[a,1,2], David L. K. Toner[b,1], Sarah K. Hodge[a], Ramon Grima[b], and Andrew J. Millar[a,b,3]

[a]School of Biological Sciences, University of Edinburgh, Edinburgh EH9 3JH, United Kingdom; and [b]SynthSys, Edinburgh EH9 3JD, United Kingdom

Edited by Philip N. Benfey, Duke University, Durham, NC, and approved March 9, 2012 (received for review November 17, 2011)

The circadian clocks that drive daily rhythms in animals are tightly coupled among the cells of some tissues. The coupling profoundly affects cellular rhythmicity and is central to contemporary understanding of circadian physiology and behavior. In contrast, studies of the clock in plant cells have largely ignored intercellular coupling, which is reported to be very weak or absent. We used luciferase reporter gene imaging to monitor circadian rhythms in leaves of *Arabidopsis thaliana* plants, achieving resolution close to the cellular level. Leaves grown without environmental cycles for up to 3 wk reproducibly showed spatiotemporal waves of gene expression consistent with intercellular coupling, using several reporter genes. Within individual leaves, different regions differed in phase by up to 17 h. A broad range of patterns was observed among leaves, rather than a common spatial distribution of circadian properties. Leaves exposed to light–dark cycles always had fully synchronized rhythms, which could desynchronize rapidly. After 4 d in constant light, some leaves were as desynchronized as leaves grown without any rhythmic input. Applying light–dark cycles to such a leaf resulted in full synchronization within 2–4 d. Thus, the rhythms of all cells were coupled to external light–dark cycles far more strongly than the cellular clocks were coupled to each other. Spontaneous desynchronization under constant conditions was limited, consistent with weak intercellular coupling among heterogeneous clocks. Both the weakness of coupling and the heterogeneity among cells are relevant to interpret molecular studies and to understand the physiological functions of the plant circadian clock.

intercellular signaling | coupled oscillators | systems biology | plant physiology | gene regulatory networks

As most habitats are characterized by 24-h day–night cycles and seasonal changes, endogenous circadian rhythms are important for organisms to anticipate and adapt to their environment. In plants, the circadian clock regulates biological processes including rhythmic leaf movement, hormone responses, Ca^{2+} concentrations, and stomatal opening (1). Interlocked transcriptional–translational feedback loops are required to sustain robust rhythms. In *Arabidopsis*, current models for these feedback loops incorporate morning-expressed genes including *CIRCADIAN CLOCK ASSOCIATED 1* (*CCA1*) and *LATE ELONGATED HYPOCOTYL* (*LHY*), which repress evening-expressed genes such as *TIMING OF CAB EXPRESSION 1* (*TOC1*) and *GIGANTEA* (*GI*), within a more complex circuit (2). Biochemical studies of the clock mechanism measure the average circuit behavior but have hardly investigated spatial patterns of rhythmicity.

Imaging assays of rhythmic *LUCIFERASE* (*LUC*) reporter genes allowed noninvasive readouts with spatial resolution (3), showing that individual cells support autonomous circadian oscillators (4, 5). The coupling of clocks among cells is now a topic of intense interest, because dynamical systems theory shows that such coupling can profoundly alter the period and entrainment behavior of multioscillator systems (6, 7). The mammalian suprachiasmatic nucleus (SCN) has been most studied: Tight coupling by synaptic transmission among SCN neurons is crucial to sustain rhythmicity (7, 8). Heterogeneity among individual neurons leads to spatiotemporal waves of rhythmic gene expression in SCN slice cultures (9–11).

In contrast, clocks in plant cells appeared to be coupled much more weakly, if at all. Different rhythmic markers spontaneously desynchronize under constant conditions, as shown for the free-running periods of cytosolic free calcium and light-harvesting complex (*LHCB*) gene expression in tobacco (12) or the expression of *LHCB* and other reporter genes in *Arabidopsis thaliana* (13, 14). These results derived from whole-plant assays and were interpreted as showing desynchronization among the different cell types that express the distinct markers. Furthermore, plants can be experimentally desynchronized, using light–dark treatments to different locations of the same plant. After transfer to constant light, these regions showed little relative phase change within time series of up to 5 d (5) and hence no evidence of coupling among cells expressing the same *LUC* marker, although longer time series suggested weak coupling (15).

We developed imaging and analysis methods to investigate circadian coupling in short time series of *LUC* reporter gene expression in plant leaves. Circadian rhythms became desynchronized among cells in constant light conditions. Their desynchronization was limited by the emergence of spatiotemporal patterns, so circadian time was never randomized across the leaf. We therefore tested the importance of intercellular coupling relative to synchronization by the light–dark (LD) cycle and show that light entrainment dominates plant circadian behavior in laboratory conditions.

Results

Setup and Analysis. To monitor luminescence rhythms in plants over several days, a protocol was designed to image healthy leaves of intact transgenic seedlings for up to 6 d (Fig. S1 and Fig. 1 *B* and *C*). Imaging of detached leaves, similarly to ref. 15, allowed us to test expression rhythms in older, isolated tissue (Fig. 1*A*). Luminescence time series were obtained from 24, 12-d-old seedlings or 8, 21-d-old detached leaves in a single field of view in the imaging cabinet with tissue-level resolution (image pixel size 230 μm, Fig. 1*C*) or from a single leaf with cellular resolution in the microscope (pixel size 5 μm, Fig. 1*D* and Movie S1). Here we focus on tissue-level data with relatively high signal levels. Preliminary time series for the control marker *35S:LUC* confirmed that the signal from plants in imaging cabinets was strong enough to analyze not only the leaf average but also single pixels (Fig. S1 *C* and *D*).

Author contributions: B.W., S.K.H., and A.J.M. designed research; B.W. and S.K.H. performed research; D.L.K.T. and R.G. contributed new reagents/analytic tools; D.L.K.T. and R.G. analyzed data; and B.W., D.L.K.T., and A.J.M. wrote the paper.

The authors declare no conflict of interest.

This article is a PNAS Direct Submission.

Freely available online through the PNAS open access option.

[1]B.W. and D.L.K.T. contributed equally to this work.

[2]Present address: Institut National de la Recherche Agronomique, Unité de Recherche 419, Unité de Recherche sur les Espèces Fruitières, Centre de Bordeaux, F-33140 Villenave d'Ornon Cedex, France.

[3]To whom correspondence should be addressed. E-mail: Andrew.Millar@ed.ac.uk.

This article contains supporting information online at www.pnas.org/lookup/suppl/doi:10.1073/pnas.1118814109/-/DCSupplemental.

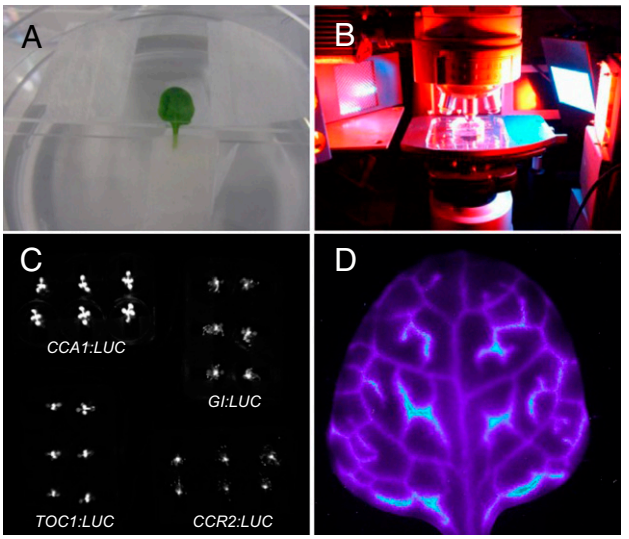

Fig. 1. Setup for imaging luciferase in intact and detached leaves over several days. (*A*) Setup for one detached leaf; (*B*) red and blue light-emitting diode (LED) system for intact plant imaging under the microscope; (*C*) luminescence output for four six-well plates as imaged in a cabinet; (*D*) luminescence output in pseudocolor from a *CCA1:LUC* leaf imaged (25×) as in *B*. Movie S1 shows the time series from a similar leaf.

Loss of Spatial Synchronization in Leaves Without Entrainment. Most circadian studies on seedlings have averaged the luminescence signal across the whole seedling or leaf, in plants grown under LD cycles and then transferred to constant light (LL) for imaging. However, our pixel-level analysis showed that such averaging masks significant heterogeneity (Fig. 2 *A* and *B*). Similar heterogeneity was observed for multiple circadian clock markers, including *GI:LUC* (Fig. S2*A*) and *CCR2:LUC* (Fig. S2*B*).

To assess the spatial organization of circadian rhythms across the leaf, rhythmic *CCA1:LUC* luminescence data (Fig. 2 *B* and *C*) were processed to identify the circadian phase at the single-pixel level (*Materials and Methods* and Fig. S3). Spatial variation in rhythmic amplitude had no consistent effect (Fig. S4). The calculated phases were used to generate image sequences, termed phase maps (Fig. 2*D*). The circadian period of this leaf increased in LL conditions [first peak at ZT2, second at ZT28, and third at ZT56, where time is measured as Zeitgeber time (ZT) in hours since the last dark–light transition]. In a synchronized leaf all leaf areas are expected to be at the same phase and hence shown in the same color, but here (Fig. 2*D*), as early as ZT22 at least three colors are present in the map, already indicating a range of different phases. A spatiotemporal pattern was clear at ZT48 (Fig. 2*E*). Along the midline, the leaf tip phase led the leaf base by >1.5 h. This loss of spatial synchronization was also observed with *GI:LUC* and *CCR2:LUC* markers (Fig. S2 *C–F*). The *CCA1:LUC* marker is used below, because its high luminescence signals allowed the most precise analysis. Table S1 presents an index of all plants analyzed.

To analyze these patterns quantitatively, the directional statistics measure of mean resultant length (16), *R*, was used to evaluate the degree of phase "coherence" among the leaf oscillators at each time point, t_k. *N* is the sample size of pixels:

$$R(t_k) = \frac{1}{N(t_k)} \left| \sum e^{i\theta_n(t_k)} \right|.$$

R takes values near 0 when phase values of the oscillators are widely dispersed on the unit circle and near 1 when the phases are tightly clustered or coherent (Fig. 3*A* and *SI Materials and Methods*).

As expected, *R* values for both intact and detached leaves of LD-grown plants started close to 1. However, a loss of synchronization could be quantitatively observed as *R* values decreased at various rates after transfer into constant conditions, with similar behavior in intact plants (Fig. 3*B*) and detached leaves (Fig. 3*C*, Fig. S5*A*, and Movie S2). The emerging patterns were similar among some of the leaves. In the examples shown, circadian peaks started first at the leaf margins (from ZT48–50) and then spread toward the center of the blade (Fig. 3*C* and Fig. S5*A*). A similar pattern was observed in the luminescence signal by microscopy (Movie S1). The patterns strongly suggest that the circadian system is heterogeneous among *CCA1:LUC*-expressing cells. Any intercellular coupling was thus insufficient to prevent the cellular heterogeneity from desynchronizing the circadian rhythms among cells, within a few days in constant light.

Spatial Patterns of Circadian Rhythmicity Vary Among Leaves. *CCA1:LUC* expression was therefore imaged, and *R* values calculated, in leaves of nonsynchronized plants that were both grown and imaged in LL. As expected, these leaves were less synchronized and had a wide range of *R* values <1 but, surprisingly, not <0.4 (Fig. 3*B*), whereas *R* would be 0 for uniformly randomized phases. Two LD-grown leaves reached a similar level of asynchrony (*R* value) to that of LL-grown leaves within 4 d (Fig. 3*B*); the data suggest other LD-grown leaves could do so within a few more days. Phase maps showed a range of phases (colors) in LL-grown leaves but their spatial distribution was not random (Fig. 3*D*, Fig. S5 *B–D*, and Movie S3). Phase was locally coherent, within a characteristic length of ≤1 mm (Fig. S6 and *SI Materials and Methods*).

To better observe the shape of the traveling waves of *CCA1:LUC* in LL-grown plants, image sequences were constructed to map only pixels at the peak of rhythm in two independent, detached leaves (Fig. 4 *A* and *B*). The leaves had different patterns: (*i*) Early peaks started in the middle of the leaf blade and spread toward the edges (Fig. 4*A*) and (*ii*) early peaks started at the tip of the leaf and spread toward the petiole (Fig. 4*B*). The propagation speeds of the first wave from tip to petiole were 1.3 mm/h (plant 16, Fig. 4*A*) and 1.8 mm/h (plant 20, Fig. 4*B*). These spatial patterns of peak firing were sustained over four cycles, indicating some stability over time. In addition, these patterns could be linked to maps of the mean circadian period (*SI Materials and Methods*). The mean period was shown to be lower in the areas where the peaks started (period ~ 22.5 h; Fig. 4 *A*, *B*, *E*, and *F* and Fig. S7 *E–J*) and higher in the regions that the wave reached last (period ~ 24.5 h; Fig. 4 *A*, *B*, *E*, and *F* and Fig. S7 *E–J*). The calculated periods are also locally correlated (Fig. S6 *C* and *F*). Period differences reflect changing phase relationships among the leaf areas.

To investigate the range of spatial patterns among plants, heterogeneity in the mean period was compared among 34 leaves (10 detached and 24 intact) grown and imaged in LL. The period patterns of 14 leaves fell into three groups (Table S1):

i) Higher period at the leaf margins (on one side or all around the leaf), sometimes with a slight vascular pattern of increased period: 2 intact leaves, 6 detached leaves (including plant 16; Figs. 3*D* and 4*E* and Fig. S7*F*.

ii) Higher period in the central region of the leaf: 4 intact leaves (including plant 56; Fig. 4*C* and Fig. S7*B*).

iii) Higher period toward the petiole: 1 intact leaf (plant 58; Fig. 4*D* and Fig. S7*D*) and 1 detached leaf (plant 20; Fig. 4*F* and Fig. S7*I*).

Of the remaining leaves, 10 had only one circadian cycle with good quality data over the majority of the leaf and 10 had highly

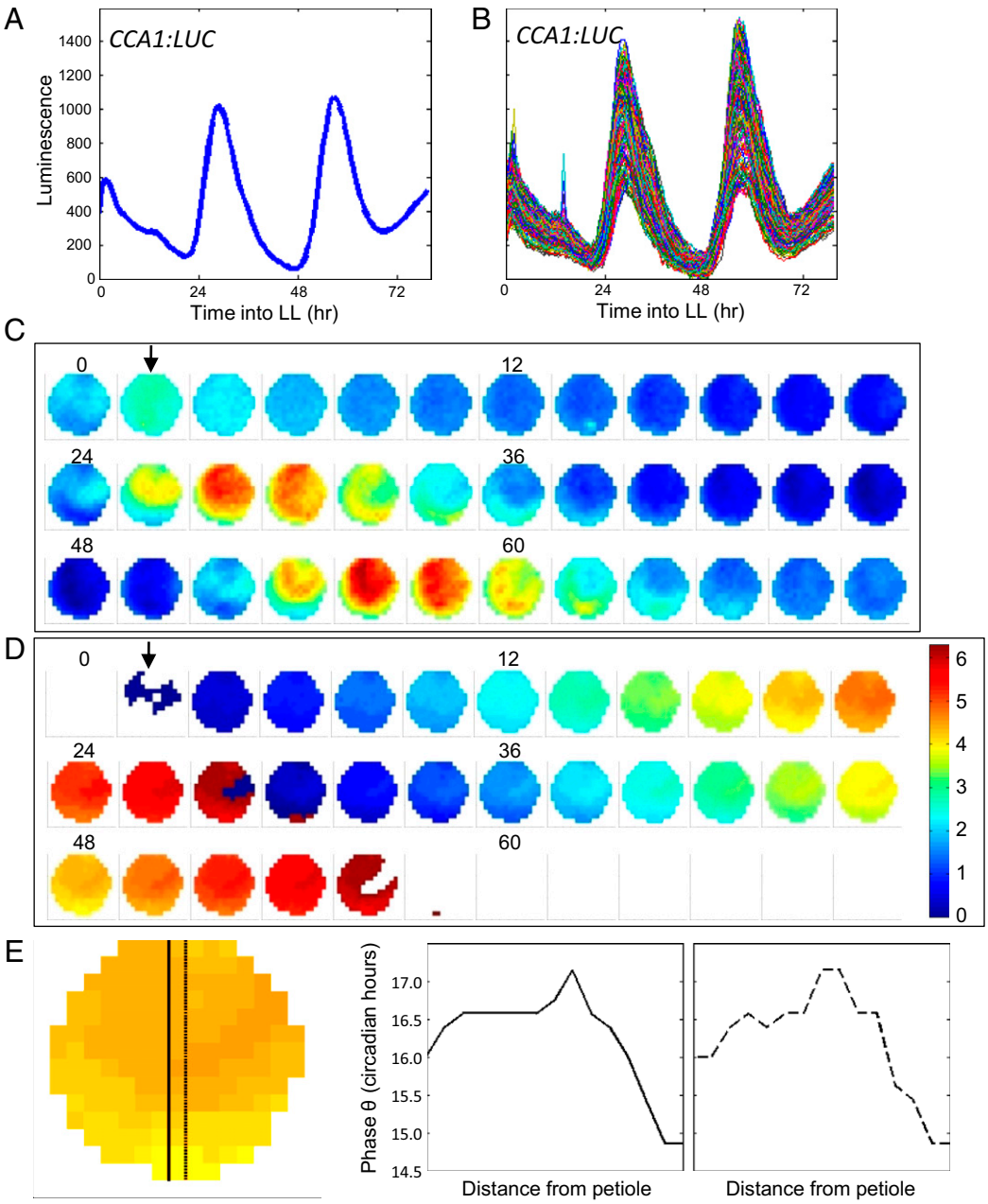

Fig. 2. Spatiotemporal analysis of *CCA1:LUC* rhythms in an intact leaf entrained under light–dark cycles and imaged under constant light. Plants were entrained under LD 12:12 cycles for 12 d and then transferred and imaged under LL conditions. (*A*) Average luminescence, detrended, for a *CCA1:LUC* leaf (Table S1, plant 23); (*B*) detrended luminescence for all pixels of the leaf in *A*; (*C*) montage showing the spatial pattern of the luminescence in *B* (interval between images = 2 h); (*D*) data in *C* represented as a montage of the circadian phase (in radians) at each pixel; (*E*) phase at ZT48 along two central lines. The phase values are at the location of the pixel values, as shown by the overlaid lines. No colored square is created for the uppermost data points, at the leaf petiole. Arrow in *C* and *D* indicates the petiole. Time is in hours; ZT0 corresponds to transfer to LL.

variable periods in some or all of the leaf, so the mean periods gave no useful conclusions.

Although phase differences within a leaf could be large (up to 17 h in plant 12), leaves never had spatially randomized phases ($R \sim 0$), consistent with a role for intercellular coupling in limiting the extent of asynchrony. The range of R values and spatial patterns of rhythmicity also suggest a dynamic system, rather than a static, spatial pattern of circadian properties among the cells of the leaf. Slowing rising or falling periods (mean absolute change 0.65 h per cycle, upper bound 2.67 h per cycle; Fig. S7 *K–M* and *SI Materials and Methods*) would progressively alter the spatial phase patterns over longer timescales than our sampling times.

Balance of Internal and External Coupling. To test how far these spatiotemporal patterns might affect circadian rhythms in nature, 23 intact, LL-grown plants were transferred to LD and imaged in cabinets. Twenty-two of 23 leaves yielded a good quality *CCA1:LUC* luminescence signal. The 4 fully analyzable leaves lost essentially all phase heterogeneity within three cycles (ZT72), as they synchronized with the LD cycle (Figs. 3*B* and 5, Fig. S8*A*, and Movie S4). The remaining 18 leaves exhibited complex multimodal expression patterns during synchronization, due to the variable starting phase and the acute light induction of the *CCA1:LUC* reporter, which hampered phase analysis. However, 16 showed near-complete synchronization within four LD cycles, as

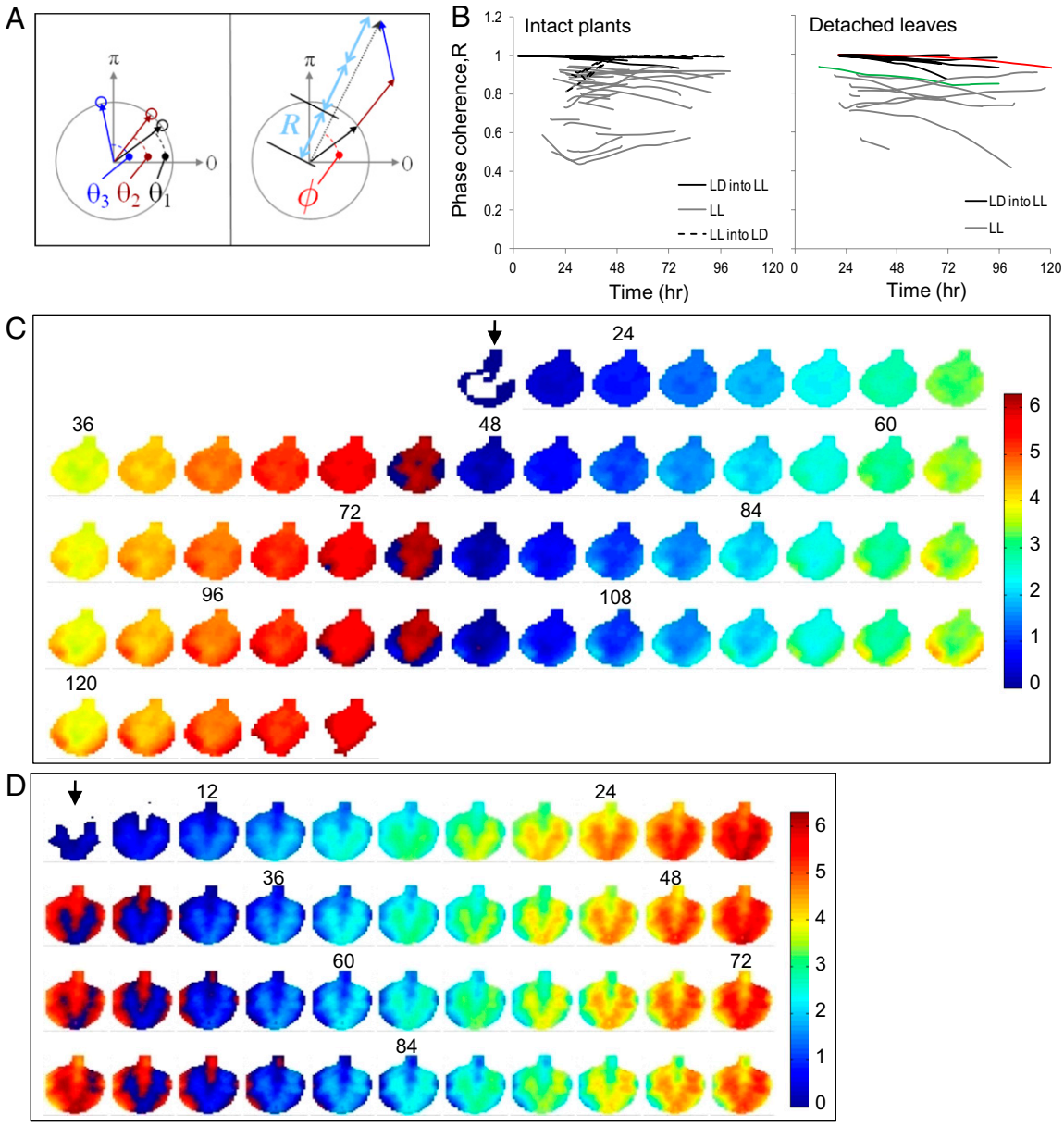

Fig. 3. Quantification of phase coherence and montages. (*A*) Calculation of phase coherence, *R*, of the phase vectors projected on the unit circle. (*Left*) At a particular time point, three pixels have phase angles θ_1, θ_2, and θ_3. Addition of the vectors and division by $n = 3$ gives the mean resultant length, *R*. In this example *R* is close to 1, showing that the phases of the three pixels are rather tightly clustered. (*Right*) ϕ indicates the mean phase at this time point. (*B*) *R* values for intact plants and detached leaves. Red and green lines represent plant 3 and plant 16, respectively (Table S1). (*C*) Phase montage for a *CCA1:LUC* detached leaf, grown in LD for 21 d and imaged in LL (Table S1, plant 3); one cycle is 28 h. (*D*) Phase montage for a *CCA1:LUC* detached leaf, grown in LL for 21 d and imaged in LL (Table S1, plant 16); one cycle is 24 h. Interval between two images = 2 h. Time is in hours; ZT0 corresponds to the start of imaging. Arrow in *C* and *D* indicates the position of the petiole.

judged by visually synchronous final peaks in the time series (Fig. S8*B*). Thus, the spatiotemporal circadian patterns of leaves in constant light are rapidly erased by entrainment to the external light/dark cycle.

Discussion

The intercellular coupling of circadian oscillators can transform the properties of the circadian system, including its flexibility and robustness. We developed a protocol to image *LUC* reporter expression in young leaves over several days, to analyze spatiotemporal patterns of clock gene expression under changing light conditions. A recent study detected desynchronization between leaf stomatal and mesophyll cells after 7 d in LL (17). Our data likely reflect multiple cell types, with mesophyll cells most numerous. Imaging their rhythms extended the recent finding, as we observed an increase in the phase heterogeneity as early as 48 h in LL. Plant-level assays commonly find falling rhythmic amplitudes in these conditions. Rising phase heterogeneity will contribute to this damping, consistent with other reports (17–19) and with recent stochastic models (20).

The maximum possible phase heterogeneity was tested in nonsynchronized plants, grown and imaged exclusively in LL. We found sustained spatiotemporal patterns of luminescence and circadian phase within the leaf, characterized by a range of phase coherence values ($R = 0.4$–0.95). In contrast, SCN slice cultures maintain $R \sim 0.85$ (10). Thus, intercellular coupling in plants was

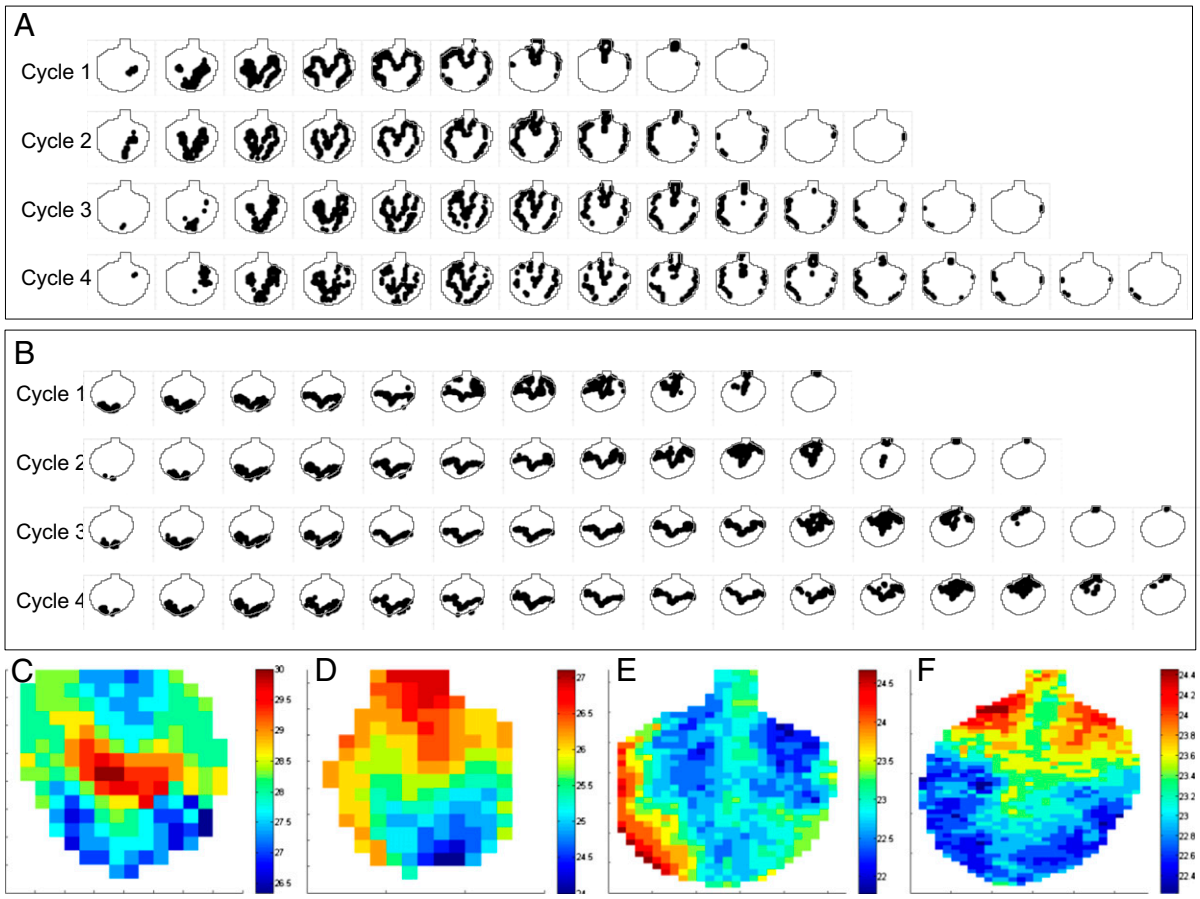

Fig. 4. Spatiotemporal patterns in plants grown and imaged under constant light. (*A* and *B*) Peak firing patterns for two independent *CCA1:LUC* detached leaves (Table S1, plants 16 and 20, respectively) grown and imaged in LL. Black dots represent the leaf areas peaking at the time of the picture. Interval between two images = 40 min. (*C* and *D*) Mean period for two independent *CCA1:LUC* intact leaves (Table S1, plants 56 and 58, respectively), grown and imaged in LL. (*E* and *F*) Mean period for the detached leaves shown in *A* and *B*. Plants were grown in LL for 21 d (*A* and *B*) or 12 d (*C* and *D*) before imaging.

too weak to maintain synchrony, but strong enough to avoid phase randomization and to promote spatiotemporal waves of circadian gene expression. This result is consistent both with the earlier studies arguing that plant cells were (at least partially) uncoupled (5, 13, 14, 17) and with results that indicated a weak but detectable coupling (15).

Regional phase differences were well documented in the SCN (7, 9) but had rarely been investigated in the leaf, except for the stomatal guard cells (17) and proposals of longer periods in the leaf vasculature (15, 21). Our joint analysis of *R* values, phase patterns, peak firing, and mean period maps revealed substantial variability among the set of leaves tested under LL, with at least

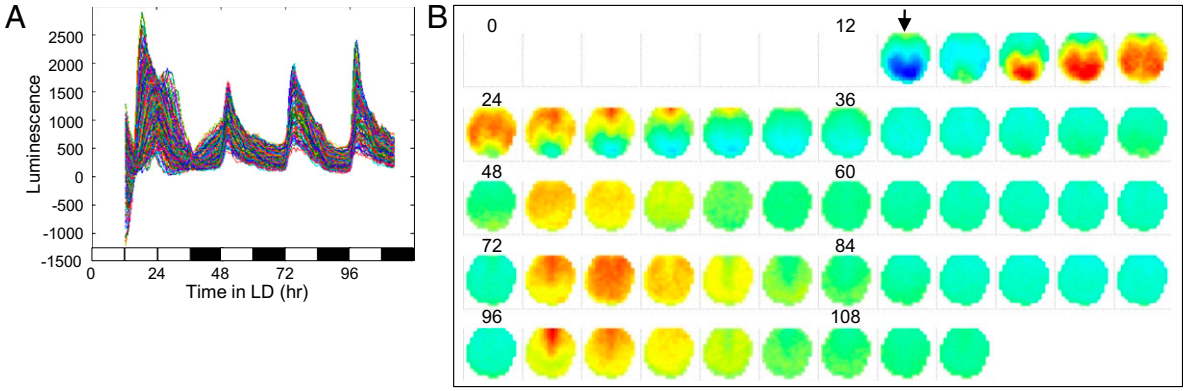

Fig. 5. Resynchronization of nonentrained leaves. Plant 31 (Table S1) was grown under LL conditions for 13 d and transferred into LL and then LD for imaging. (*A*) Luminescence for all pixels, detrended for the *CCA1:LUC* leaf. (*B*) Montage of the detrended luminescence, interval between two images = 2 h. Time is in hours; ZT0 corresponds to start of imaging. Arrow in *B* indicates the position of the petiole.

three broad spatiotemporal patterns. The changing phase coherence of individual leaves (Fig. 3*B*) suggests that a wide range of spatiotemporal patterns might be generated over time within a single leaf, by the interaction of stochastic cellular clocks with intercellular coupling. Our studies would sample from this larger set of possible dynamic patterns, which might include phenomena such as spiral waves (15) that we did not observe. This result seems at odds with suggestions that some cell types consistently have distinct circadian properties (14, 22), although these notions are not mutually exclusive. Earlier studies averaging over many leaves would likely emphasize spatial regularities, particularly if specific patterns were temporarily favored by a common experimental condition such as the transition from LD entrainment to LL (5, 17, 21).

The mechanisms of clock heterogeneity and intercellular coupling that underlie the observed patterns remain unclear. Several signaling components are known to move through the leaf and to alter the circadian clock, including the phytohormones auxin and cytokinins (23, 24), which might promote wave-like propagation of circadian phase at the rates observed. Experimental uncoupling assays, as demonstrated in the SCN (11), and models of cell arrays (10) will be essential to further investigate these hypotheses and to test their relevance to any natural condition in the leaf. Our results from LD entrainment or reentrainment show that light–dark cues are more important than intracellular coupling in synchronizing the clocks of leaf cells. Cell types with less direct access to light may still entrain to chemical proxies for light (such as sugars) that are communicated among cells (22, 25). It remains possible that some plant cells beyond the range of even indirect light signals rely on intercellular circadian coupling, of the type we measure here among leaf cells.

Materials and Methods

Plant Material and Growth Conditions. The *35S:LUC*, *CCA1:LUC+*, *GI:LUC+*, and *CCR2:LUC+* lines in the *Wassilewskija* accession have been described (26, 27). Seeds were surface sterilized, sown on Gilroy-agar media [no added sucrose, 1.5% (wt/vol) agar], and stratified at 4 °C for 96 h in darkness. Seedlings were then grown at 22 °C under LL conditions or (12 h/12 h) LD cycles of 75 $\mu mol \cdot m^{-2} \cdot s^{-1}$ cool white fluorescent light for 11 d (intact plants) or 20 d (detached leaves) in Sanyo MLR350 environmental test chambers.

Imaging Protocol. Eleven-day-old intact leaves and 20-d-old detached leaves were kept healthy between a slide and a coverslip and kept immobile both horizontally and vertically (Fig. S1 *A* and *B* and Fig. 1*A*), as detailed in *SI Materials and Methods*. Leaves were treated with luciferin before imaging and provided with a liquid Murashige and Skoog (MS) solution and luciferin during imaging. Luminescence images were captured as described in ref. 27.

Data Processing. Luminescence images were analyzed for a square array of pixels containing a leaf and surrounding area, as detailed in *SI Materials and Methods*. Briefly, numerical data for each leaf were processed to locate the data peaks and define each pixel's time-dependent phase, $\theta_n(t)$. For each pixel, n, we use the definition of time-varying phase as a piecewise linear function between successive peak times T^k and T^{k+1}, as used by Fukuda et al. (15); i.e.,

$$\theta_n(t) = 2\pi \frac{t - T_n^k}{T_n^{k+1} - T_n^k}, \quad t \in [T_n^k, T_n^{k+1}).$$

Nonleaf pixels were removed using signal quality measures, a process that involved data detrending. Peaks of the detrended data were located using the *findpeaks* function in MATLAB (Mathworks), with the aid of digital filters to reject local fluctuations in the data. Period means and SDs (or alternatively the period range when the number of periods $n = 2$) were calculated for each pixel, where periods are defined as the set of peak-to-peak times for that pixel.

ACKNOWLEDGMENTS. We thank a reviewer for helpful suggestions. B.W. was supported by Institut National de la Recherche Agronomique, France. D.L.K.T. and R.G. were supported by the Scottish Universities Life Sciences Alliance. Experimental work was supported by the European Commission Seventh Framework Programme (FP7) Collaborative Project TiMet (Project 245143) (to A.J.M. and others). SynthSys is a Center for Integrative and Systems Biology supported by Biotechnology and Biological Sciences Research Council and Engineering and Physical Sciences Research Council Award D019621.

1. McWatters HG, Devlin PF (2011) Timing in plants—a rhythmic arrangement. *FEBS Lett* 585:1474–1484.
2. Pokhilko A, et al. (2012) The clock gene circuit in Arabidopsis includes a repressilator with additional feedback loops. *Mol Syst Biol* 8:574.
3. Millar AJ, Short SR, Chua NH, Kay SA (1992) A novel circadian phenotype based on firefly luciferase expression in transgenic plants. *Plant Cell* 4:1075–1087.
4. Plautz JD, Kaneko M, Hall JC, Kay SA (1997) Independent photoreceptive circadian clocks throughout Drosophila. *Science* 278:1632–1635.
5. Thain SC, Hall A, Millar AJ (2000) Functional independence of circadian clocks that regulate plant gene expression. *Curr Biol* 10:951–956.
6. Strogatz SH (2001) Exploring complex networks. *Nature* 410:268–276.
7. Welsh DK, Takahashi JS, Kay SA (2010) Suprachiasmatic nucleus: Cell autonomy and network properties. *Annu Rev Physiol* 72:551–577.
8. Aton SJ, Herzog ED (2005) Come together, right. . .now: Synchronization of rhythms in a mammalian circadian clock. *Neuron* 48:531–534.
9. Evans JA, Leise TL, Castanon-Cervantes O, Davidson AJ (2011) Intrinsic regulation of spatiotemporal organization within the suprachiasmatic nucleus. *PLoS ONE* 6:e15869.
10. Fukuda H, Tokuda I, Hashimoto S, Hayasaka N (2011) Quantitative analysis of phase wave of gene expression in the mammalian central circadian clock network. *PLoS ONE* 6:e23568.
11. Yamaguchi S, et al. (2003) Synchronization of cellular clocks in the suprachiasmatic nucleus. *Science* 302:1408–1412.
12. Sai J, Johnson CH (1999) Different circadian oscillators control Ca(2+) fluxes and lhcb gene expression. *Proc Natl Acad Sci USA* 96:11659–11663.
13. Hall A, Kozma-Bognár L, Bastow RM, Nagy F, Millar AJ (2002) Distinct regulation of CAB and PHYB gene expression by similar circadian clocks. *Plant J* 32:529–537.
14. Thain SC, Murtas G, Lynn JR, McGrath RB, Millar AJ (2002) The circadian clock that controls gene expression in Arabidopsis is tissue specific. *Plant Physiol* 130:102–110.
15. Fukuda H, Nakamichi N, Hisatsune M, Murase H, Mizuno T (2007) Synchronization of plant circadian oscillators with a phase delay effect of the vein network. *Phys Rev Lett* 99:098102.
16. Mardia KV, Jupp PE (2000) *Directional Statistics* (Wiley, New York), pp 15–18.
17. Yakir E, et al. (2011) Cell autonomous and cell-type specific circadian rhythms in Arabidopsis. *Plant J* 68:520–531.
18. Hall A, Kozma-Bognár L, Tóth R, Nagy F, Millar AJ (2001) Conditional circadian regulation of PHYTOCHROME A gene expression. *Plant Physiol* 127:1808–1818.
19. Rascher U, et al. (2001) Spatiotemporal variation of metabolism in a plant circadian rhythm: The biological clock as an assembly of coupled individual oscillators. *Proc Natl Acad Sci USA* 98:11801–11805.
20. Guerriero ML, et al. (2012) Stochastic properties of the plant circadian clock. *J R Soc Interface* 9:744–756.
21. Para A, et al. (2007) PRR3 is a vascular regulator of TOC1 stability in the Arabidopsis circadian clock. *Plant Cell* 19:3462–3473.
22. James AB, et al. (2008) The circadian clock in Arabidopsis roots is a simplified slave version of the clock in shoots. *Science* 322:1832–1835.
23. Covington MF, Harmer SL (2007) The circadian clock regulates auxin signaling and responses in Arabidopsis. *PLoS Biol* 5:e222.
24. Hanano S, Domagalska MA, Nagy F, Davis SJ (2006) Multiple phytohormones influence distinct parameters of the plant circadian clock. *Genes Cells* 11:1381–1392.
25. Bischoff F, Millar AJ, Kay SA, Furuya M (1997) Phytochrome-induced intercellular signalling activates *cab*: luciferase gene expression. *Plant J* 12:839–849.
26. Doyle MR, et al. (2002) The ELF4 gene controls circadian rhythms and flowering time in Arabidopsis thaliana. *Nature* 419:74–77.
27. Edwards KD, et al. (2010) Quantitative analysis of regulatory flexibility under changing environmental conditions. *Mol Syst Biol* 6:424.